March 1990

LAPP-TH-277
CERN-TH-5639/90

Quark Flavours and the γ-Ray Spectrum from Halo Dark Matter Annihilations

Hans-Uno Bengtsson[ab], Pierre Salati[cd] * and Joseph Silk[d]

a) Physics Department, University of California at Los Angeles.
b) Department of Theoretical Physics, University of Lund.
c) Theory Division, CERN.
d) Center for Particle Astrophysics and Astronomy Department, University of California at Berkeley.

Abstract

An indirect signature for the presence of exotic particles in the dark halo of our galaxy is the γ-ray flux produced by their annihilations. The cold dark matter (CDM) species annihilate into $q\overline{q}$ and $\tau^+\tau^-$ pairs which subsequently hadronize. Using the Lund Monte Carlo, we have systematically simulated the fragmentation of back-to-back quark and antiquark jets and analyzed the resulting π^0 and γ-ray spectra for various energies and flavours. Scaling of these spectra obtains for a jet energy $M_\chi > 10$ GeV. Jets involving heavy flavours give softer spectra than light quarks. We provide analytic fits of the π^0 and photon spectra which may be combined with the annihilation branching ratios of any CDM candidate model to predict the halo γ-ray signal. Provided they annihilate mostly into light quarks and τ leptons, species lighter than ~ 50 GeV may be detected by a GRO type γ-ray telescope exposed up to a month to high galactic latitudes. We finally investigate the possibility of a clumpy halo where $\sim 1\%$ of the mass concentrates in substructures of typical scale $10^8\, M_\odot$. Would a 1° angular resolution telescope detect hot spots in the γ-ray sky at high and intermediate galactic latitudes, this would be a "smoking gun" for the presence of clumps of exotic matter inside the halo.

---

*On leave of absence from LAPP, BP110, 74941 Annecy-le-Vieux Cedex, France and Université de Chambéry, 73000 Chambéry, France.

1 - Introduction.

A significant fraction of the mass of the universe is invisible. Flat galactic rotation curves and the dynamics of clusters of galaxies [1,2] indicate the presence of dark matter. The problem has been known for a long time [3] but only recently have people considered the exciting possibility of an exotic nature for the dark matter. Theoretical arguments (*i.e.*, inflation predicts $\Omega = 1$) when combined with the fact that $\Omega_{\rm baryon}$ cannot exceed ~ 0.2 (primordial nucleosynthesis) suggest that 90% of the matter in the universe is non-baryonic. If so, our own galactic halo may be composed of relic particles left over during the Big Bang. A favoured candidate for the dark matter is a weakly interacting massive species (WIMP) with typical scattering cross section off nuclei $\sigma_{\chi N} \sim 10^{-36}\,{\rm cm}^2$ and mass $M_\chi \sim 1 - 100$ GeV.

These cold dark matter (CDM) particles may be detected directly. Since they collide with nuclei, they can deposit energy inside bolometers or ionize semi-conductors [4,5]. A dark matter detector using germanium [6] has already ruled out the interval 9–12 GeV $< M_\chi < 1$ TeV if the CDM candidates have neutrino-like interactions. More sensitive experiments such as silicon detectors or ultra-low temperature bolometers based on phonons [7] or rotons [8] detection should be able to rule out (or to detect) WIMPs. CDM particles could also be detected indirectly. If actually they comprise the galactic halo, they are continuously accreted by stars and concentrate in their cores where they may eventually control the energy transport. Several authors have argued that these CDM species may solve the solar neutrino puzzle [9]. They can also suppress convection inside low mass main sequence stars [10] and induce thermal pulses of horizontal branch stars [11].

Another possibility is the annihilations of the CDM particles inside our galactic halo. The associated high energy γ-ray signal is potentially detectable. If the CDM species annihilate into $q\overline{q}$ pairs, the subsequent hadronization of the jets produces π^0, η, η', D^*, ω, etc... These mesons may in turn decay radiatively so that for each intermediate $q\overline{q}$ configuration, a specific photon spectrum emerges :

$$\chi\overline{\chi} \rightarrow q\overline{q} \rightarrow (\pi^0, \eta, ...) \rightarrow \gamma + Y \ . \qquad (1)$$

Two main steps are necessary in order to estimate the γ-ray spectrum for a given CDM candidate :

• The branching ratios of the various hadronic channels $\chi\overline{\chi} \rightarrow q\overline{q}$ are specified for each CDM candidate. Note that the χ particles annihilate at rest ($v_\chi \sim 300\,{\rm km\,s^{-1}}$), so that the quark and antiquark jets are back-to-back. Each model gives its own specific mixture of heavy and light quarks and of τ leptons.

• The hadronization pattern of an initial back-to-back $q\overline{q}$ state leads to a unique photon spectrum. Here, the theory of jet fragmentation comes into play.

In order to reproduce the photon yield of each jet, the first calculations of the CDM γ-ray signature [12,13] made actually use of the e^+e^- collider data. More refined treatments have been presented in the same spirit [14,15] but only recently have Monte Carlo simulations of jet fragmentation been used in order to derive the annihilation γ-ray signal [16,17,18]. However these analyses have never been systematic. The most refined treatment [17] only provides the spectra dN_γ/dE_γ for the c and b quarks and the τ lepton for a jet energy $\sqrt{s}/2 = M_\chi = 10$ GeV. We have therefore analyzed the γ-ray production by CDM annihilation more thoroughly.

In section 2, we investigate the photon spectrum produced by the hadronization of an initial back-to-back quark and antiquark jet configuration. Jet fragmentation is modelled by the Lund Monte Carlo and each simulation runs over 10^5 events, a significant statistical sample. For each quark flavour and for the τ, the jet energy (*i.e.*, the mass M_χ of the initial CDM particle) is varied from 2.5 to 80 GeV. The γ spectra are shown to scale with energy above $M_\chi \sim 10$ GeV and to be softer for heavy flavours. Photons are mostly produced by pion decays. In the scaling regime ($\sqrt{s}/2 =$ 80 GeV), the π^0 and γ spectra may be conveniently approximated by the expression $dN/dx = A\,e^{-\alpha x} + B\,e^{-\beta x}$ so that fits may be easily combined with the various annihilation branching ratios of any CDM model to predict the resulting halo γ-ray signature. In section 3 we discuss the γ-ray signal produced by a generic candidate which annihilates only into a single flavour. For a closure relic density, the CDM γ-ray signal is $\sim$ an order of magnitude below the galactic disk background, provided the main annihilation channels only involve light quarks (u and d) or τ leptons. If so, a GRO type γ-ray telescope needs to be exposed to high galactic latitude at least a month in order to detect particles with mass $M_\chi < 50$ GeV. If the χ annihilations mostly produce heavy quarks such as the top, the γ-ray signal is further reduced. Finally, we explore in section 4 the possibility of a clumpy structure for the galactic halo with $\sim 1\%$ of the dark matter forming overconcentrations with typical scale $\sim 10^8\,M_\odot$ and density $\rho_{clump} \sim (1 + z_{clump})^3\,\rho_{halo} \sim 10^3\,\rho_{halo}$. Such CDM remnants of the formation of the galactic halo could be detected by satellite or space station borne telescopes as hot spots in the γ-ray sky at high and intermediate galactic latitudes.

2 - Quark flavours and the pion and gamma spectra.

The Lund Monte Carlo for Jet Fragmentation, JETSET version 6.3 [19], used here is a Monte Carlo implementation of the Lund model for string fragmentation [20]. The given references contain most of the physics that go into the Monte Carlo program; here, it is sufficient to remark that in the string picture, when a quark and an antiquark forming a colour singlet move out back-to-back, they stretch between them a narrow tube containing the colour field. The dynamics of this system can be modelled mathematically by the relativistic, massless string. If the quark and antiquark are sufficiently energetic, at some point it becomes energetically favourable for the colour field to break, producing new quark-antiquark pairs. The colour singlet systems resulting from a sequence of such break-ups are, in the Lund model, thought to be the final state hadrons. This leads to an iterative recipe for the hadron cascade suited for implementation in a computer program. The primary hadrons created from the string-breaking are then allowed to decay into stable particles according to measured branching ratios - this is also done inside the program, which further contains treatment of gluon radiation, etc. The program has been extremely successful in describing e^+e^- data; combined with other event generators, it has also been favourably tested against hadron collider data.

The all-dominating source of γ is the decay $\pi^0 \to 2\gamma$; thus an understanding of the π^0-spectrum produced in the fragmentation and subsequent decay of the string systems will also suffice to explain the final γ-spectrum. This is explicitly seen in Fig. 3a–3b, where the π^0 derived (short-dashed) and the γ (solid) spectra are compared for u-quark and b-quark systems, respectively. Combining the π^0 spectra (dotted) with the radiative pion decays yields a signal

$$\frac{dN_\gamma}{dx} = \int_{x_{inf}}^{1} \left(\frac{dN_{\pi^0}}{dy}\right) \frac{2}{\sqrt{y^2 - a^2}}\, dy \ , \qquad (2)$$

where $x = E_\gamma/M_\setminus$, $y = E_{\pi^0}/M_\setminus$, $a = m_{\pi^0}/M_\setminus$ and the lower bound on the integral is $x_{inf} = x + a^2/4x$. Fig. 1a–1f show the expected scaling properties, i.e. the γ spectrum depends only on the scaled variable $x = E_\gamma/M_\setminus$. This is of course just a reflection of the underlying assumption of scaling in the fragmentation model itself, plus, as noted, the fact that the γ come predominantly from π^0 decay. In Fig.2a–2b we compare the γ spectra from fragmentation of different quark flavours at two energies. We note that the spectra become increasingly softer as the quark mass increases; this is easily understood when we consider that the lighter flavours (u, d) can give rise to leading π^0's, and thus γ's with a large fraction of the total available energy, whereas heavy flavours will only

produce π^0's further down the fragmentation chain, or from decay of the heavy leading hadrons, both of which will give π^0's (and thus γ's) at lower x-values.

This difference is further elaborated on in Figs 4a–4b. When the string breaks, it will produce quark-antiquark pairs in the ratio u:d:s $\approx$ 1:1:0.3 (these values are fitted from comparisons with e^+e^- data); no heavier quarks are produced in the fragmentation (see [20,19] for a discussion of this statement). Once the leading particles are removed from the fragmentation chain, the systems will essentially look the same, irrespective of leading quark flavour (this statement neglects effects of the different masses of the leading hadrons produced). Differences in the π^0 spectra should thus mainly be attributable to leading particle effects. u and d quark fragmentation will give rise to leading π^0's (and thus γ's), whereas other quark flavours will not. s quark fragmentation will give rise to leading K's and K^*'s. As can be seen from the particle data tables, decay of these will only give π^0's a small fraction of the time. $s\bar{s}$ systems will thus have fewer π^0's than $u\bar{u}$ and $d\bar{d}$ systems; the energy fraction carried by π^0's (and γ's) will also be smaller for fragmenting $s\bar{s}$ systems (the π^0's come from further down the fragmentation chain). For $c\bar{c}$ and $b\bar{b}$ systems this conclusion is modified as follows. Since these systems will have leading heavy hadrons that decay with a rather large hadron multiplicity, the number of π^0's produced will in general be as large as or larger than for $u\bar{u}$ and $d\bar{d}$ systems (we once again refer to the particle data tables); however, the π^0's will each carry only a small fraction of the leading particle energy, so that the total energy fraction carried by π^0's in these cases is smaller than for the light quark systems. This is clearly seen in Fig. 4a, where at any given energy of the fragmenting system, b-quarks produce more π^0's (and thus γ's) than c-quarks, which in turn produce more π^0's than u and d (these two give the same, as they should, since π^0 is an equal mixture of $u\bar{u}$ and $d\bar{d}$). s-quarks are also seen to produce fewer π^0's than u's and d's, quite in accordance with the above discussion. In Fig. 4b is plotted the total energy fraction carried by γ's for different endpoint quarks; here, u and d give rise to a larger energy fraction carried by the γ's than b and c, which is also in agreement with the above: as stated, the energy of the π^0's in b and c fragmentation will be degraded, since many of the π^0's here come from decay of leading heavy hadrons. The energy fraction carried by the π^0's (or γ's) for an $s\bar{s}$ system remains the lowest.

We finally conclude this section with a pedestrian approach of the fact that for u and d quark systems, a third of the initial energy is degraded into π^0's (and consequently into γ's). Let us focus on the leading π^0 emerging from a u quark jet. The u quark has roughly equal probability to get dressed with a $\bar{u}$ or a $\bar{d}$ quark.

• A $u\bar{u}$ system has therefore an equal probability of 1/4 to end up as a π^0 or a ρ^0. In the latter case, the leading particle will not be a pion since the reaction $\rho^0 \to 2\,\pi^0$ is forbidden while the predominant decay channel is $\rho^0 \to \pi^+\pi^-$.

• A $u\bar{d}$ system has also an equal probability of 1/4 to give a π^+ (in which case the leading particle is the charged pion and not the π^0), or a ρ^+ which mainly decays into π^0 and π^+. In the latter case, the fraction of the jet energy carried by π^0's will be 1/8.

Adding up the various π^0 contributions, we find that 3/8 of the energy carried by leading particles appears as π^0's. Note that the subsequent fragmentation of the string obeys the same rules so that we end up with an energy fraction carried by π^0's of $\sim 37.5\%$. This energy fraction should be furthermore decreased by a factor $\sim 2/2.3$ since we have neglected string fragmentation into $s\bar{s}$ systems which yield much less π^0's. Combining these arguments leads to an energy fraction $\approx 33\%$, in good agreement with Fig. 4a.

3 - The γ-ray spectrum from halo dark matter annihilations.

3.1 - The annihilation signal.

The γ-ray flux on earth generated by the galactic halo dark matter annihilations is a function of the integral along the line of sight of the particle density squared, and depends on the specific γ-ray spectrum generated by the annihilations :

$$I_\gamma = \frac{\langle\sigma_A v\rangle}{4\pi}\bigg|_{tot} \left(\frac{dN_\gamma}{dE_\gamma}\right) \int_{\text{line of sight}} n_\chi^2\, dL \ . \qquad (3)$$

This flux is expressed in units of $\text{cm}^{-2}\,\text{s}^{-1}\,\text{sr}^{-1}\,\text{GeV}^{-1}$.

In this section, we assume a spheroidal distribution for the halo CDM particles and will explore later on the effects of possible clumpiness. The particle density at galactocentric distance r is given in terms of its solar neighbourhood value $n_\chi(\odot)$:

$$n_\chi(r) = n_\chi(\odot) \left(\frac{a^2 + r_\odot^2}{a^2 + r^2}\right) \ , \qquad (4)$$

where a denotes the core radius of the CDM halo. The integral along the line of sight may be performed analytically [21,22] and leads to

$$\int_{\text{line of sight}} n_\chi^2\, dL = r_\odot\, n_\chi^2(\odot)\, \mathcal{J}(b,l) \ , \qquad (5)$$

where $\mathcal{J}(b,l)$ is a function of galactic longitude l and galactic latitude b. Denoting the ratio $r_\odot/a$ by α and defining the parameter β as :

$$\beta^2 = 1 + \alpha^2\,(1 - \cos^2 b \cos^2 l) \ , \qquad (6)$$

leads to the expression :

$$\mathcal{J}(b,l) = \frac{(1+\alpha^2)^2}{2\alpha\beta^3} \left\{\frac{\pi}{2} + \frac{\alpha\beta}{1+\alpha^2}\cos b \cos l + \tan^{-1}\left(\frac{\alpha}{\beta}\cos l \cos b\right)\right\} \ . \qquad (7)$$

The behaviour of $\mathcal{J}(b,l)$ as a function of the only relevant parameter (cosb cosl) is presented in Fig. 5, for three different values of α : 1/2, 1 and 2. Note that the largest signal originates from the galactic center, *i.e.*, (cosb cosl) = 1 while it is minimum in the anticentric direction (cosb cosl) = -1. The disk contribution to the background is minimum in the direction of the galactic pole so that we will now concentrate on the special value (cosb cosl) = 0. In this case, the line of sight integral simplifies into :

$$\mathcal{J}(b,l) = \frac{\pi\beta}{4a} \ . \qquad (8)$$

Whenever a numerical value is needed, we set $r_\odot = 8.5$ kpc and $a = 7$ kpc, hence $\mathcal{J}(b = 90^\circ) \simeq 1.02$.

The γ-ray spectrum arising from the CDM particle annihilations is a convolution of the annihilation cross-sections with the relevant photon spectra over the various fermion-antifermion channels. The results of the Lund Monte-Carlo discussed in the previous section naturally appear by defining :

$$\langle\sigma_A v\rangle_{tot} \left(\frac{dN_\gamma}{dE_\gamma}\right) = \sum_{f\bar{f}\ \text{channels}} \sigma_A v(\chi\bar{\chi} \to f\bar{f}) \left(\frac{dN_\gamma}{dE_\gamma}\right)_{f\bar{f}} \qquad (9)$$

in relation (3). The expected signal may therefore be expressed as

$$I_\gamma = 3.4 \times 10^{-6}\,(\text{cm}^{-2}\,\text{s}^{-1}\,\text{sr}^{-1}\,\text{GeV}^{-1}) \left(\frac{\rho_\chi}{0.4\,\text{GeV cm}^{-3}}\right)^2 \left(\frac{1\,\text{GeV}}{M_\chi}\right)^2 \times$$
$$\times \sum_{f\bar{f}\ \text{channels}} \left\{\frac{\sigma_A v(\chi\bar{\chi} \to f\bar{f})}{10^{-26}\,\text{cm}^3\,\text{s}^{-1}}\right\} \left(\frac{dN_\gamma}{dE_\gamma}\right)_{f\bar{f}} \ . \qquad (10)$$

The CDM mass density ρ_χ has been set equal to $0.43\,\text{GeV cm}^{-3}$ in our numerical estimates. Before discussing the results, we briefly present the background to the CDM annihilation signal.

3.2 - The background.

This background is not known in the energy range 1-100 GeV. We must extrapolate from lower energy data taken by the satellites SAS-2 and COS-B. The SAS-2 experiment had no sensitivity above 0.2 GeV but is the only one to give information on the flux at high galactic latitude and from extragalactic sources. The COS-B experiment [23] measured a diffuse *galactic* γ-ray flux at low and intermediate galactic latitudes, its highest energy channel being 0.8-6 GeV. Below $\sim$ 300 MeV, we have taken the background to be :

$$B_\gamma = 2.8 \times 10^{-6} \, (\mathrm{cm^{-2}\, s^{-1}\, sr^{-1}\, GeV^{-1}}) \left(\frac{E_\gamma}{1\ \mathrm{GeV}}\right)^{-1.6} . \qquad (11)$$

To predict the expected background above $\sim$ 300 MeV, one therefore has to extrapolate over a considerable energy range and to model the various contributions to the background. The γ-rays of galactic origin either come from point sources (such as the Crab or Vela pulsars) or from a diffuse component due to the bremsstrahlung of cosmic ray electrons or to the decays of π^0's produced by collisions of cosmic ray protons on interstellar gas. The latter mechanism is the dominant contribution above 1 GeV. Extragalactic γ-rays also come from point sources (active galactic nuclei) or from a diffuse component, the origin of which is not well understood (unresolved point sources, or cosmological origin ?). The observed galactic plane diffuse γ-ray emissivity is found to correlate well with the total gas column density. This supports the interpretation of the observed diffuse flux as primarily being due to cosmic ray interactions (mainly π^0 production in the COS-B energy range) with interstellar atoms [24]. There are also small contributions from relativistic electron bremsstrahlung, which scales with the interstellar gas column density, and from inverse Compton emission by relativistic electron scattering in the diffuse galactic radiation field. Analysis of the COS-B data yields an empirical diffuse galactic γ-ray emissivity of $4 \times 10^{-27} \mathrm{s^{-1} sr^{-1} (H_{atom})^{-1}}$ in the 300-800 MeV range, and $2 \times 10^{-27} \mathrm{s^{-1} sr^{-1} (H_{atom})^{-1}}$ over 800 MeV-6 GeV. The inferred spectral dependence is approximately proportional to $E^{-2.7}$ [25] :

$$B_\gamma = 8.0 \times 10^{-7} \, (\mathrm{cm^{-2}\, s^{-1}\, sr^{-1}\, GeV^{-1}}) \left(\frac{E_\gamma}{1\ \mathrm{GeV}}\right)^{-2.7} . \qquad (12)$$

The extra-galactic background is not well known, and different analyses do not agree on the extrapolation of COS-B and SAS-2 measurements to energies larger than 1 GeV [26]. Since it may drop sharply above 1 GeV, we do not consider it any further, but keep in mind the possibility that it could be of the same order of magnitude as the galactic background.

3.3 - The γ-ray spectrum.

Some candidates such as the photino or the higgsino predominantly annihilate into heavy quarks. On the contrary, heavy neutrinos (*i.e.*, $M_\chi > 46$ GeV) have several annihilation channels with roughly similar branching ratios. In order to understand the effect of quark flavours on the annihilation γ-ray signal, we investigate the case of a generic CDM particle which annihilates only into a single fermion-antifermion channel. Figure 6a (resp. 6b and 6c) presents the case of a particle with mass $M_\chi = 5$ GeV (resp. 20 and 80 GeV). The annihilation at rest of this species has been derived from its cosmological relic abundance, assuming for simplicity that the annihilation cross-section at decoupling, during the early stages of the universe, and now in the galactic halo, are the same. The relic abundance Ωh^2 implies a value

$$\sigma_A v \simeq 1.8 \times 10^{-27} \, \mathrm{cm^3 s^{-1}} \left(\Omega h^2\right)^{-1} , \qquad (13)$$

for the annihilation cross-section. Each plot displays the case of a CDM species annihilating *only* into d quarks (dotted), τ leptons (short-dash) or the heaviest possible channel allowed by the kinematics of the annihilation reaction (solid). This heaviest quark is the charm for $M_\chi = 5$ GeV (Fig. 6a), the bottom for $M_\chi = 20$ GeV (Fig. 6b) and the top for $M_\chi = 80$ GeV (Fig. 6c). Several remarks are in order :

- As implied by relation 2, the γ-ray spectra have a maximum for $E_\gamma = m_{\pi^0}/2$ and are symmetric in logarithmic scale around that value.

- The d and τ channels give similar spectra above $E_\gamma \sim M_\chi/4$ while heavy quarks produce a much softer signal. Heavy quarks carry a significant fraction of the jet energy and also tend, on the average, to fragmentate more. The net result is the production of many low energy photons and the depletion relative to lighter species of the high energy tail of the γ-ray spectrum. This effect is most apparent in Fig. 6c where the top mass is 60 GeV while $M_\chi = 80$ GeV : for $E_\gamma \sim$ 20–40 GeV, the d and τ spectra are comparable to the background with a flux of order 10^{-10} cm^{-2} s^{-1} sr^{-1} GeV^{-1} (note that $\Omega h^2 = 1/40$), whereas for a pure top annihilation, the signal is two orders of magnitude fainter.

- For τ leptons, the low energy part of the γ-ray spectrum is significantly reduced with respect to the quark cases.

- As implied by relation (13), the smaller the relic density, the larger the CDM annihilation cross-section and the signal. In Fig. 6a, spectra corresponding to $\Omega h^2 = 1/40$ slightly stand above background for γ-ray energies in the range 500 MeV–3 GeV. For somewhat larger values of the relic density, say $\Omega h^2 = 1/4$, the d and τ spectra are

now an order of magnitude below background. Fig. 6b and 6c exhibit similar features. We therefore keep in mind that for light quarks and τ's, the signal-to-background ratio is maximum around $E_\gamma \sim M_\chi/3$ and is of order unity for $\Omega h^2 \approx 1/40$, irrespective of the mass M_χ. If on the one hand the annihilation flux I_γ behaves as M_χ^{-3} (assuming pure scaling of the photon spectra dN_γ/dx), on the other hand, the background B_γ decreases as $E_\gamma^{-2.7}$ so that the signal-to-background ratio is fairly insensitive to M_χ.

• We therefore suggest that scanning with respect to galactic latitude of the γ-ray signal around $E_\gamma \sim M_\chi/3$ is a worthwhile method to extract the annihilation signal from the disk background. Spectral distortions with respect to measurements averaged over a significant fraction of the sky (say, $45° < b < 90°$) should be present in that energy range. However, the CDM annihilation signal should be, at least, larger than the typical 1σ error associated with the measurements, *i.e.*,

$$\text{Noise} \approx \sqrt{N} < \left(\frac{1/40}{\Omega h^2}\right) N \approx \text{CDM Signal} \ , \tag{14}$$

where N denotes the number of photons accumulated in the energy bins of interest. The galactic disk provides the dominant contribution to the γ-ray signal so that for a GRO type γ-ray telescope [27] with a 1 m^2 sr effective area and a $\Delta E/E = 10\%$ energy resolution, the daily statistics involve

$$N \approx 450 \,\text{photons/day} \ \left(\frac{1\,GeV}{M_\chi}\right)^{1.7} \ . \tag{15}$$

Sensitivity to the γ-ray annihilation signal therefore requires that the effective exposure time T_{exp} of the detector to high galactic latitudes should exceed

$$T_{exp} > 3.5 \,\text{days} \ \left(\Omega h^2\right)^2 \left(\frac{M_\chi}{1\,GeV}\right)^{1.7} \ . \tag{16}$$

Assuming that an entire month seems to be an upper limit (Note that GRO is scheduled to operate during 7 effective days), a halo dark matter particle can be detected provided

$$M_\chi < 3.5 \,\text{GeV} \ \left(\Omega h^2\right)^{-1.2} \ . \tag{17}$$

For realistic values of the relic density, *i.e.*, $\Omega h^2 \sim 0.1$–1, CDM candidates to the halo dark matter are detectable up to $M_\chi \sim 50$ GeV. Heavier species require considerably larger detector areas or much longer exposure times since the γ-ray signal is fainter at high energy and, if heavy channels open up, the signal-to-background ratio decreases significantly due to a much softer spectrum.

• Finally, the HI distribution in the galactic disk has been observed [28] to be patchy. An approximate 1% of the sky is covered with regions towards which the HI column

density is lower than $0.9 \times 10^{20}\,cm^{-2}$. Since the galactic diffuse background correlates well with the total gas column density, it has been suggested [29] that the CDM γ-ray signal should be explored inside these HI holes in which the signal-to-background ratio would be enhanced with respect to average. However, the γ-ray telescope should have a good angular resolution ($< 1°$) and a fairly large effective area in order to collect a statistically significant sample of photons out of the HI holes. The problem is further complicated by the presence of an extra-galactic background with which the interesting signal from halo dark matter may be mixed up.

As an illustration, we present in Fig. 7 the case of the photino $\tilde{\gamma}$, the neutral spin 1/2 Majorana fermion associated to the photon by supersymmetry. This particle may annihilate into $f\overline{f}$ pairs through the exchange of the spin-0 supersymmetric partners $\tilde{f}_R$ and $\tilde{f}_L$ of the fermion f. For simplicity, we assume the same generic mass $\tilde{M}$ for all the sfermion species whatever their chirality. The annihilation cross section depends on the photino mass $M_{\tilde{\gamma}}$

$$\begin{aligned} \sigma v_{rel}(\tilde{\gamma}\tilde{\gamma} \to f\overline{f}) \ &= \ 8\pi\alpha^2 \frac{Q_f^4}{\tilde{M}^4} M_{\tilde{\gamma}}{}^2 \sqrt{1-z_f^2} \times \\ &\times \ \left\{ z_f^2 + \frac{\beta_{\rm rel}^2}{3}\left(1 - \frac{7}{4}z_f^2 + \frac{3}{8}\frac{z_f^4}{1-z_f^2}\right)\right\} \ , \end{aligned} \tag{18}$$

where α is the fine structure constant, Q_f and m_f are the electric charge (in units of the proton charge) and the mass of the fermion f, and z_f is the ratio $m_f/M_{\tilde{\gamma}}$. Each figure displays three values for the photino relic abundance : $\Omega h^2 = 1/40$, 1/4 and 1. The Lund (dotted) and the π^0-derived (solid) spectra are in fairly good agreement as explained in section 2. Since halo photinos are cold, *i.e.*, $\beta_{\tilde{\gamma}} \sim 10^{-3}$, the annihilation cross section responsible for the CDM γ-ray signal evolves like $Q_f^4 m_f^2$. The various annihilation channels are in the sequence $c : \tau : b : t = 1 : 7 : 0.7 : 100$. For the two configurations of Fig. 7a and 7b for which $M_{\tilde{\gamma}} = 5$ and 20 GeV, the dominant annihilation channel is the τ so that the γ-ray spectra are fairly similar to the τ curves (short dash) of Fig. 6a in the high energy regime while they reproduce the b and c cases (solid) for low energy photons. Furthermore, specifying the photino relic density determines the annihilation cross section *at decoupling* and not its present and somewhat reduced value. The various spectra displayed in Fig. 7 are therefore shifted downwards by a factor $\sigma v_{now}/\sigma v_{dec}$ with respect to the generic examples of Fig. 6. This shift is most apparent in Fig. 7b for $M_{\tilde{\gamma}} = 20$ GeV. Finally, a heavy photino annihilates mostly into $t\overline{t}$, hence the soft γ-ray spectrum of Fig. 7c which reproduces fairly well the solid curve of Fig. 6c.

The photino examplifies the general procedure to determine the γ-ray spectrum orig-

inating from dark matter annihilations in the halo. For each candidate, the annihilation cross section at decoupling, during the early universe, and now, in the halo, are determined by specifying the cosmological relic abundance of the dark matter species. For a spheroidal halo, relation (10) combines the γ-ray spectra of Table 1 with the specific annihilation branching ratios of the model. We have systematically worked out in this analysis the basic ingredients, *i.e.*, the π^0 and γ-ray spectra, of a cocktail which one is now free to mix up according to some special recipe.

4 - An indirect signature of a clumpy halo.

Uniformity of the cold dark matter distribution is by no means assured even within our galactic halo. The linear fluctuation spectrum is almost flat on subgalactic scales [30], and so non-linearity occurs almost simultaneously over a wide variety of mass scales at a redshift, in the standard CDM model, $1 + z_{nl} \approx 30/b$, where the bias factor b is the ratio of the rms galaxy count fluctuations on scale $8h^{-1}$ Mpc (equal to unity) to the rms dark matter fluctuations. It is actually the deviations from a flat spectrum that determine survival probabilities when larger scales go nonlinear. Of course, truly isolated inhomogeneities survive, but we are interested here in any residual substructure in our massive halo. Evidently, provided that a given scale develops sufficient nonlinear density contrast before being incorporated into a larger scale fluctuation that is collapsing around it, the substructure is likely, at least initially, to survive tidal disruption.

We quantify this argument as follows [31]. The CDM fluctuation spectrum may be described by the power spectrum $|\delta_k|^2 \propto k^{n_{eff}}$ with an effective spectral index n_{eff} that equals the scale-invariant value of unity on large scales (>> 10 Mpc) and approaches - 3 as $k \rightarrow \infty$. However the logarithmic deviation from the - 3 value is critical here : for example at $10^6\, M_\odot$, n_{eff} = - 2.5, and at $10^{10}\, M_\odot$, n_{eff} = - 2.2. In terms of turn-around time, $t \propto M^{(n_{eff}+3)/4}$. It is apparent that relatively rare and isolated fluctuations at, say, the 2σ level are able to undergo significant collapse if M is not too small, before being incorporated into larger scales. Specifically, survival against tidal disruption and drag by dynamical friction requires a density contrast of > 100 relative to the surroundings. If we consider successive scales distinguished by a factor of 2 in filter scale, initial survival is then likely if $n_{eff} > -2.4$. This yields a surviving minimum mass of about $10^8\, M_\odot$. The above argument should be appropriate for 2σ fluctuations which happen to be roughly a factor 2 smaller than the rms fluctuation (or filter) scale. About 10% of the mass is present in 2σ fluctuations. Moreover, nonhomologous collapse with a resulting

density profile that may even be as flat as $\rho \propto r^{-2}$ would still leave about 10% of the initial clump mass trapped in the clump cores at a density enhancement (relative to that at turn-around) of about 100. We conclude that about 1% of the mass should survive in substructure of characteristic scale of order $10^8\, M_\odot$ during the early hierarchical mass condensation sequence of CDM.

Next, we consider the survival of such CDM clumps in our halo, subject to interaction with the galactic disk and spheroid. Orbital passage through the inner galaxy tends to heat the clump dark matter, most of which has only completed part of an internal orbit within the clump during the timescale over which the external gravitational field is undergoing significant variation. These "gravitational shocks" are a major contributor to destruction of globular star clusters [32], and consequently of CDM clumps. Very massive clumps are also subject to dynamical friction over a time-scale $(M_{bulge}/M_{clump})\, t_{orbit}$, so that clumps with mass $< 10^8\, M_\odot$ are relatively imune from this destruction process. Gravitational shocking by the bulge (or disk) imparts an energy per unit mass to a clump of order [33]

$$\Delta E \sim < r_{clump} >^2 \left(\frac{2GM_{bulge}}{v_{clump}\, R_{peri}^2} \right)^2 , \qquad (19)$$

where R_{peri} is the perigalacticon distance of the clump orbit, v_{clump} is the mean clump velocity, M_{bulge} is the spheroid (or disk mass) interior to the clump orbit, and $< r_{clump} >$ is a mean clump radius. We have suppressed a dimensionless form factor of order unity that depends on the extended mass distribution of the clump, and a dimensionless efficiency factor that involves the ratio of the finite encounter time with spheroid (or disk) to the internal orbit time in the clump. The inferred destruction time-scale of a clump is

$$t_{dest}/t_{orbit} \approx 4 \times 10^4 \left(\frac{10\ pc}{< r_{clump} >} \right)^2 \left(\frac{R_{peri}}{8\ kpc} \right)^2 \left(\frac{v_{clump}}{100\ km\ s^{-1}} \right)^2 \times$$
$$\times \left(\frac{10^{10}\, M_\odot}{M_{bulge}\,(R_{peri})} \right)^2 \left(\frac{M_{clump}}{10^6\, M_\odot} \right) . \qquad (20)$$

Numerical simulations have been performed for the orbits of $\sim$ 100 globular clusters (of typical mass $5 \times 10^5\, M_\odot$ and radius 5 pc) allowing for gravitational shocking by disk and bulge as well as evaporation losses, to infer a destruction rate for *present* globular cluster parameters of about $\nu_{dest}^{gc} \sim 10^{-11}\, yr^{-1}$ [34]. Scaling to CDM clumps in our dark halo, we infer a clump destruction rate

$$\nu_{dest}^{clump} \sim \left(\frac{M_{gc}}{M_{clump}} \right)^{1/3} \left(\frac{\rho_{gc}}{\rho_{clump}} \right)^{2/3} \nu_{dest}^{gc} . \qquad (21)$$

Hence with our preferred clump density value $\rho_{clump} \sim (1+z_{clump})^3 \rho_{halo}$ (as compared to $\rho_{gc}(<r>) \sim 10\, M_\odot\, pc^{-3} \sim 10^3\, \rho_{halo}$ near the sun), the rate of clump destruction is

$$\nu_{dest}^{clump} \sim 10^{-11} \left(\frac{10^6\, M_\odot}{M_{clump}}\right)^{1/3} \text{yr}^{-1} \ . \tag{22}$$

Provided that $M_{clump} > 10^4\, M_\odot$, clump destruction is unimportant via dynamical processes over the past 10^{10} years. Clumps in the inner few kpc of the Galaxy would have suffered considerable destruction : most clumps, in the outer halo, survive essentially intact.

If a fraction $f_{clump} \sim 1\%$ of the halo is in the form of CDM clumps with typical density $\rho_{clump} \sim 10^3\, \rho_{halo}$, the annihilation γ-ray signal produced in these substructures is, on average, $10^3 \times f_{clump} \sim 10$ times larger than the flux from the homogeneous component. Therefore clumpiness generates, on average, a γ-ray signal enhanced by $\sim$ an order of magnitude with respect to a purely homogeneous halo, hence a signal comparable, at least for high galactic latitudes, to the disk background. If halo CDM clusters on typical scale $M_{clump} \sim 10^8\, M_\odot$, the probability for a clump to be at distance d from the solar system is unity for

$$d \sim 10^4 \left(\frac{M_{clump}}{10^8\, M_\odot}\right)^{1/3} \left(\frac{0.01}{f_{clump}}\right)^{1/3} \text{pc} \ . \tag{23}$$

Since their typical radius is

$$< r_{clump} > \sim 130 \left(\frac{M_{clump}}{10^8\, M_\odot}\right)^{1/3} \text{pc} \ , \tag{24}$$

the angular extension in the sky of nearby clumps is

$$\theta \sim 1^\circ - 2^\circ \left(\frac{f_{clump}}{0.01}\right)^{1/3} \ , \tag{25}$$

independent of their mass. The γ-ray signal originating from these $\sim 1^\circ \times 1^\circ$ CDM concentrations is enhanced with respect to the homogeneous component by a factor

$$\frac{\text{I}_\gamma(clump)}{\text{I}_\gamma(halo)} = \frac{\int_{clump} n_\chi^2\, dL}{\int_{halo} n_\chi^2\, dL} \approx \frac{2}{\mathcal{J}(\text{b,l})} \left(\frac{< r_{clump} >}{r_\odot}\right) \left(\frac{\rho_{clump}}{\rho_{halo}}\right)^2 \ . \tag{26}$$

For typical $10^8\, M_\odot$ clumps, this contrast is $\sim 3 \times 10^4$ so that the γ-ray signal from clustered CDM is 3 orders of magnitude above the galactic disk background. A γ-ray telescope with a 1° angular resolution will therefore be able to detect nearby CDM

clumps, even if they hide at fairly low galactic latitudes. Note that COMPTEL [27] on GRO has an angular resolution $\Delta\theta = 40' - 1^\circ$ depending on the photon energy. Detection of hot spots on the γ-ray sky at various galactic latitudes would be of considerable interest and would signal the presence of exotic dark matter inside our galactic halo.

Acknowledgements : P.S. would like to express his gratitude towards D. Cline and M. Jura for their hospitality and financial support during his stay at the University of California at Los Angeles where this work was initiated.

References

[1] J. Kormandy and G.R. Knapp, IAU Symposium 117, *Dark Matter in the Universe* (1987) ed. Reidel.

[2] L.S. The and S. White, *Astron. J.* **95** (1988) No. 1, 15.

[3] F. Zwicky, *Helv. Phys. Acta* **6** (1933) 110.

[4] J. Primack, D. Seckel and B. Sadoulet, *Ann. Rev. Nucl. Part. Phys.* **38** (1988) 751.

[5] P.F. Smith and J.D. Lewin, Report Rutherford RAL-88-045 (1988).

[6] D.O. Caldwell *et al.*, *Phys. Rev. Lett.* **61** (1988) 510.

[7] B. Sadoulet in *Proceedings of the XXIIIrd Rencontres de Moriond, Les Arcs, Savoie, France, March 1988*, eds. J. Audouze and J. Tran Thanh Van, 63.

[8] R.E. Lanou, H.J. Maris and G.M. Seidel in *Proceedings of the XXIIIrd Rencontres de Moriond, Les Arcs, Savoie, France, March 1988*, eds. J. Audouze and J. Tran Thanh Van, 75.

[9] G. Steigman, C.L. Sarazin, H. Quintana and J. Faulkner, *Ap. J.* **83** (1978) 1050; D.N. Spergel and W.H. Press, *Ap. J.* **294** (1985) 663; L.M. Krauss, preprint Harvard HUTP-85/A005a (1985); J. Faulkner and R.L. Gilliland, *Ap. J.* **299** (1985) 994; R.L. Gilliland, J. Faulkner, W.H. Press and D.N. Spergel, *Ap. J.* **306** (1985) 703 and more recently Y. Giraud-Heraud, J. Kaplan, F. Martin de Volnay, C. Tao and S. Turck-Chièze, report PAR-LPTHE 89-24 (1989).

[10] A. Bouquet and P. Salati, *Ap. J.* **346** (1989) 284.

[11] D. Dearborn, G. Raffelt, P. Salati, J. Silk and A. Bouquet, reports CfPA-TH-89-008, CfPA-TH-89-009 and CfPA-TH-89-012, (1989).

[12] F.W. Stecker, S. Rudaz and T.F. Walsh, *Phys. Rev. Lett.* **55** (1985) 2622.

[13] S. Rudaz and F.W. Stecker, *Ap. J.* **325** (1988) 16.

[14] F.W. Stecker, *Phys. Lett.* **B201** (1988) 529.

[15] K. Freeze and J. Silk, preprint UCB-Astronomy (1988).

[16] A.J. Tylka and D. Eichler, unpublished (1987).

[17] J. Ellis, R.A. Flores, K. Freeze, S. Ritz, D. Seckel and J. Silk, *Phys. Lett.* **B214** (1988) 403.

[18] F.W. Stecker and A.J. Tylka, report LHEA/TH-88-46 (1988).

[19] T. Sjöstrand, *Computer Phys. Comm.* **39** (1986) 347; T. Sjöstrand, M. Bengtsson, *Computer Phys. Comm.* **43** (1987) 367.

[20] B. Andersson, G. Gustafson, G. Ingelman, T. Sjöstrand, *Phys. Rep.* **97** (1983) 31.

[21] J.E. Gunn, B.W. Lee, I. Lerche, D.N. Schramm and G. Steigman, *Ap. J.* **223** (1978) 1015.

[22] M. Turner, *Phys. Rev.* **D34** (1986) 1921.

[23] H.A. Mayer-Hasselwander *et al.*, *Astron. Astrophysics* **105** (1982) 164.

[24] J.B.G.M. Bloemen, *Ap. J. Lett.* **317** (1987) L15.

[25] C.D. Dermer, *Astron. Ap.* **157** (1986) 223.

[26] C.E. Fichtel and D.J. Thompson, *Astron. Astroph.* **109** (1982) 352.

[27] J.M. Ryan in *Proceedings of the Workshop on High Resolution γ-ray Cosmology, UCLA, California, November 1988*, eds. D. Cline and E. Fenyves, *Nucl. Phys. B in press.*

[28] H.E. Payne, E.E. Salpeter and Y. Terzian, *Ap. J.* **272** (1983) 540.

[29] J. Silk in *Proceedings of the Workshop on High Resolution γ-ray Cosmology, UCLA, California, November 1988*, eds. D. Cline and E. Fenyves, *Nucl. Phys. B in press.*

[30] J.M. Bardeen, J.R. Bond, N. Kaiser and A.S. Szalay, *Ap. J.* **304** (1986) 15.

[31] J. Silk and A. Stebbins, in preparation 1990.

[32] D. Chernoff, C. Kochanek and S. Shapiro, *Ap. J.* **309** (1986) 183.

[33] L. Spitzer, *Ap. J.* **127** (1958) 17.

[34] L.A. Aguilar, P. Hut and J.P. Ostriker, *Ap. J.* **335** (1988) 720.

Flavour	A	α	B	β
π^0 *from* d	306	48	14.8	5.76
π^0 *from* u	306	48	15.1	5.82
π^0 *from* s	332	57	21.5	8
π^0 *from* c	309	50	26.5	8.5
π^0 *from* b	225	28	20.1	8.9
π^0 *from* t	908	48	41	16.6
π^0 *from* τ	—	—	8.3	4.8
γ *from* d	1390	75	25.7	7.74
γ *from* u	1390	75	25.7	7.76
γ *from* s	1410	78	35.9	10.7
γ *from* c	1310	66	36.9	11
γ *from* b	1400	58	29.1	11.4
γ *from* t	1940	63	50.1	20.3
γ *from* τ	—	—	18.8	7.65

Table 1

The π^0 and γ-ray spectra corresponding to the scaling regime $\sqrt{s}/2 = M_\chi = 80$ GeV are fairly well approximated by the analytic expression $dN/dx = Ae^{-\alpha x} + Be^{-\beta x}$. The fit parameters are displayed for each flavour.

Figure captions

Figure 1 : The photon spectrum dN_γ/dE_γ is presented as a function of the jet energy fraction $x = E_\gamma/M_\chi$ for various quark flavours : down (**1a**), up (**1b**), strange (**1c**), charm (**1d**), bottom (**1e**) and top (**1f**). The Lund Monte-Carlo generates the hadronic showers and their associated photon yields from an initial back-to-back quark-antiquark configuration. Three values of the jet energy $M_\chi = \sqrt{s}/2$ are displayed : 2.5 GeV (dotted curves), 10 GeV (short dash curves) and 80 GeV (solid curves). Note that for each quark flavour, the energy scaling of the spectra is quite good.

Figure 2 : Same as previously but several γ spectra corresponding to different quark flavours are presented on the same graph : down (solid), up (long dash), strange (short dash), charm (dotted), bottom (short dash – dotted) and top (long dash – dotted). Fig. **2a** (resp. **2b**) corresponds to a jet energy of 5 GeV (resp. 80 GeV). Note that the heavier the quark, the smoother the photon spectrum and the steeper the slope. Heavy quarks have more decay channels than light quarks. The jet energy is therefore more degraded for heavy flavours than for light ones, leading to the production of more low energy photons.

Figure 3 : These diagrams display the π^0 (dotted) and γ (solid) spectra as given by the Lund Monte-Carlo. The photon spectrum resulting only from the pion decays $\pi^0 \rightarrow 2\gamma$ (short dash) is in fairly good agreement with the Lund predictions. The similarity between the Lund and the π^0-derived spectra clearly establishes that most of the photons originate from the pions produced during the hadronization process. Fig. **3a** (resp. **3b**) corresponds to an initial up (resp. bottom) jet with energy 5 GeV (resp. 80 GeV).

Figure 4 : Diagram **4a** presents the number of pions and photons produced in a single jet as a function of its energy $M_\chi = \sqrt{s}/2$, for various quark flavours. Conventions are the same as in Fig. **2a** and **2b**. Note that there is a factor ~ 2 between the π^0 and γ multiplicities for above-mentioned reasons. In graph **4b** the fraction of the initial jet energy which photons eventually carry away is also presented as a function of the jet energy. Note that for u and d jets, this fraction is $\sim 30\%$, for charm and bottom jets, it is $\sim 25\%$ while for bottom jets, photons carry only $\sim 20\%$ of the initial energy.

Figure 5 : The evolution of integral $\mathcal{J}(b, l)$ is presented as a function of cosb cosl for three different values of the ratio $\alpha = r_\odot/a$. The line of sight along which γ-ray photons are observed is defined by its galactic longitude l and galactic latitude b. Note that the galactic pole, for which the galactic disk component of the background is minimum,

corresponds to cosb cosl = 0.

Figure 6 : Various "generic" γ-ray spectra are displayed. Each case corresponds to a CDM candidate which only annihilates into a single flavour : either the heaviest possible quark (solid) or the lightest quark (dotted), *i.e.*, the down, or the τ lepton (short dash). In Fig. **6a**, $M_\chi = 5$ GeV and two values of the CDM relic abundance are presented : $\Omega h^2 = 1/40$ (upper curves) and $\Omega h^2 = 1$ (lower curves). Fig. **6b** corresponds to $M_\chi =$ 20 GeV and $\Omega h^2 = 1/4$ while in Fig. **6c**, $m_{top} = 60$ GeV, $M_\chi = 80$ GeV and $\Omega h^2 =$ 1/40.

Figure 7 : The case of the photino $\tilde{\gamma}$ is scrutinized for three different values of its mass : $M_{\tilde{\gamma}} = 5$ GeV (**7a**), 20 GeV (**7b**) and 80 GeV (**7c**). For each figure, spectra which correspond to a specific value of the photino relic abundance are presented : Ωh^2 = 1/40, 1/4 and 1. The Lund-computed γ spectra (dotted) and the π^0-derived spectra (solid) are in fairly good agreement for the above-mentioned reasons.

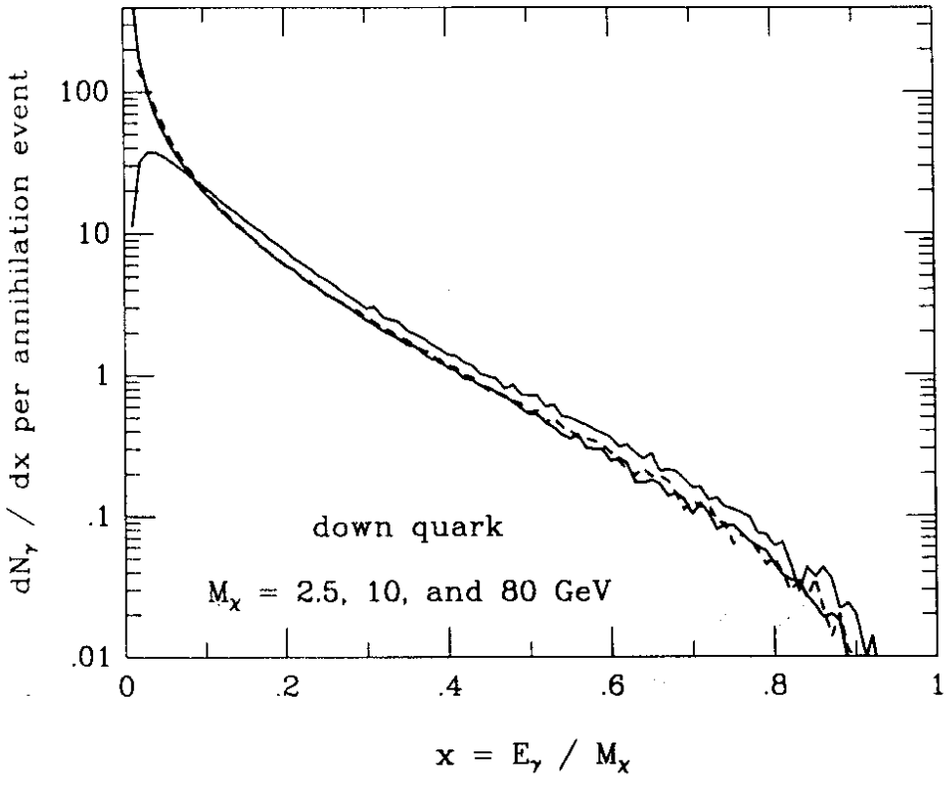

Figure 1a

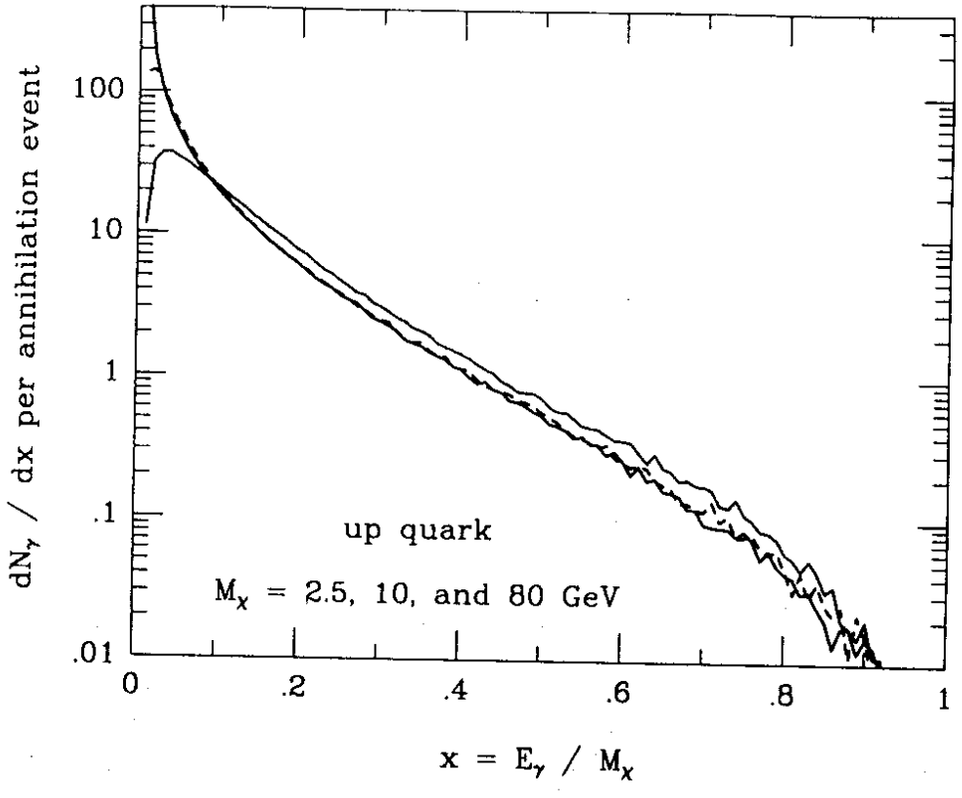

Figure 1b

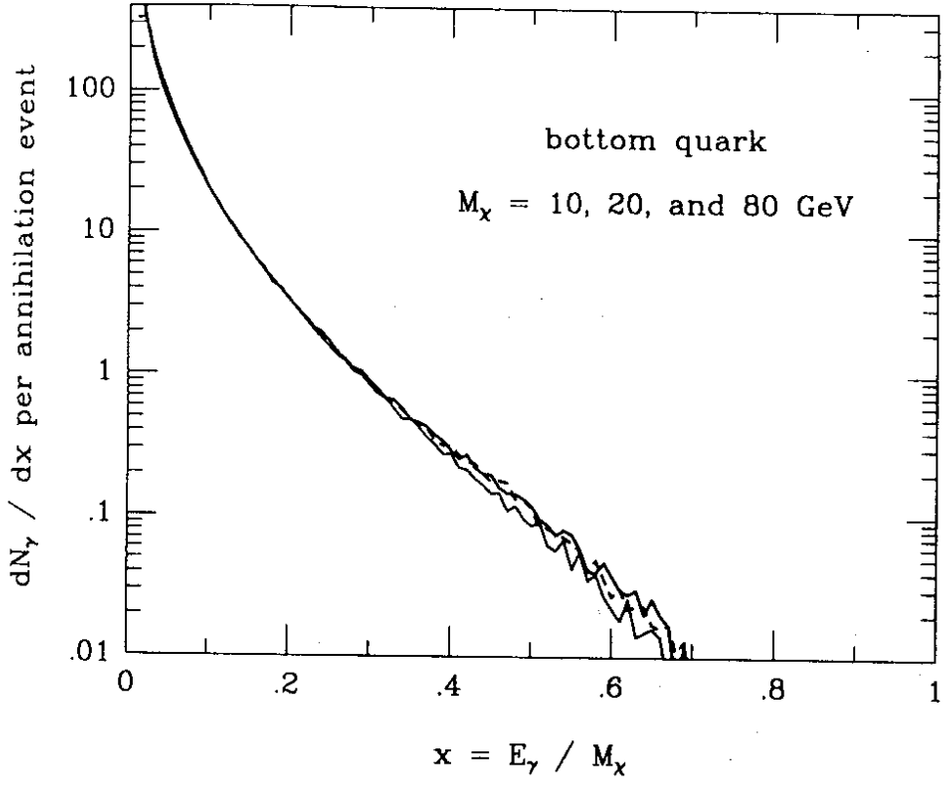

Figure 1e

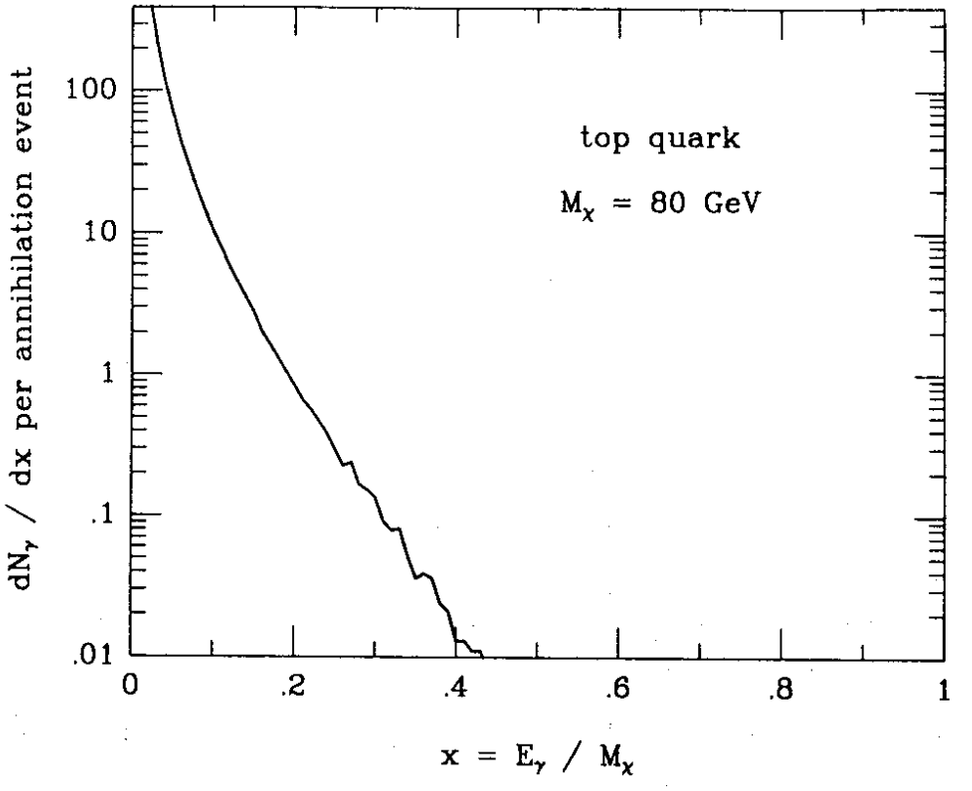

Figure 1f

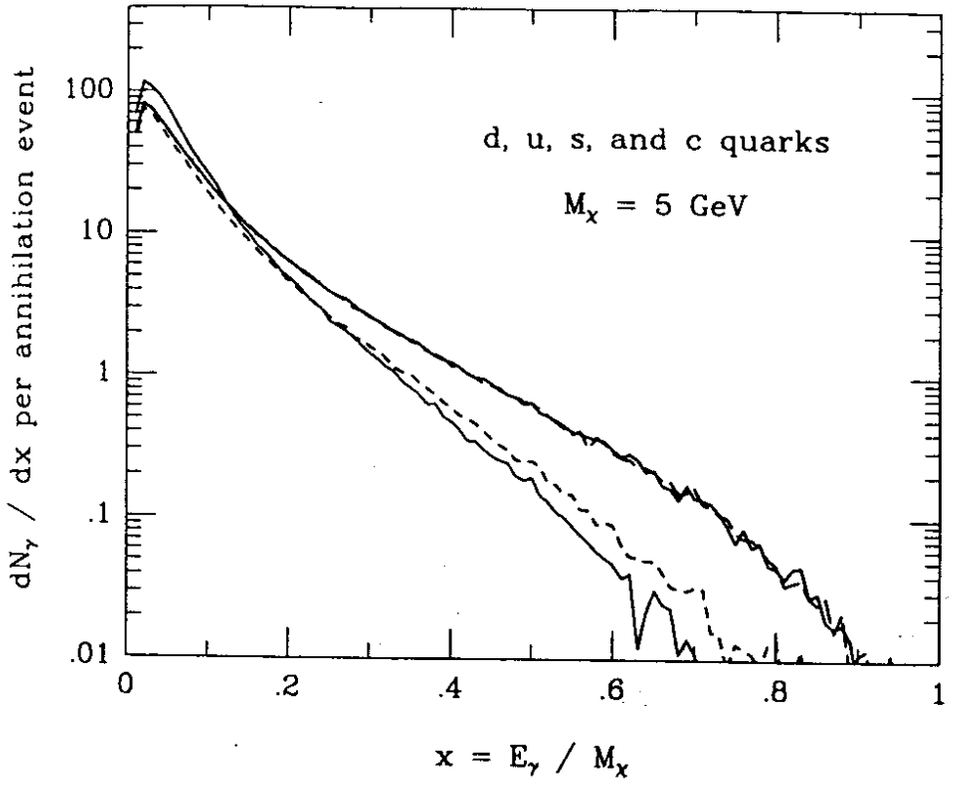

Figure 2a

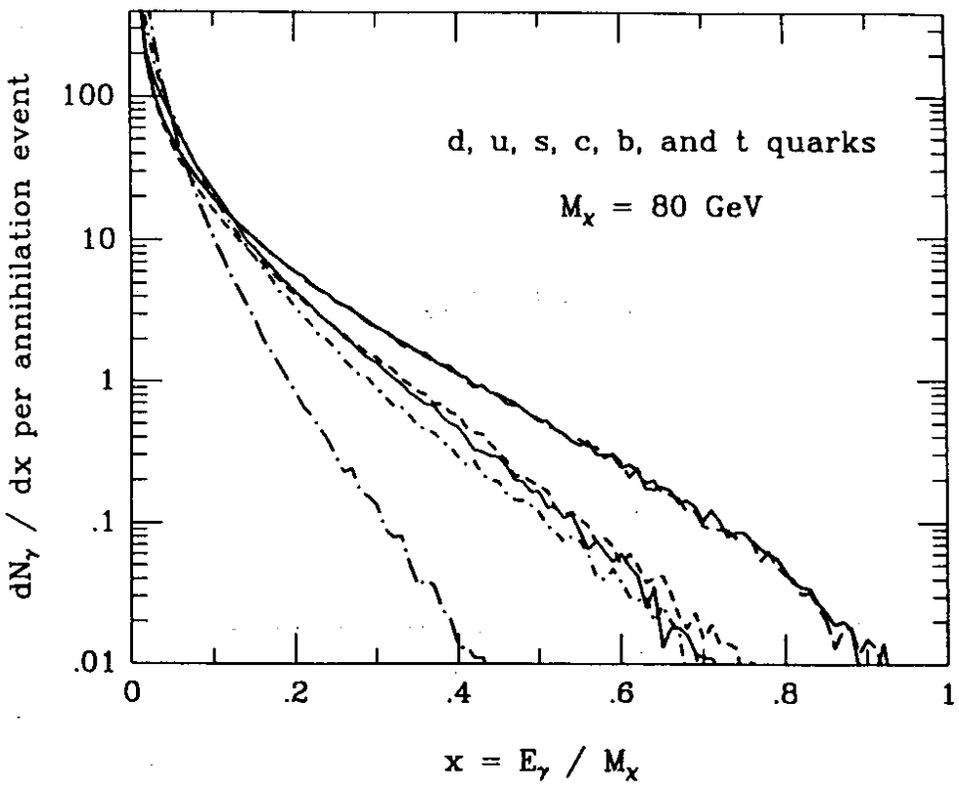

Figure 2b

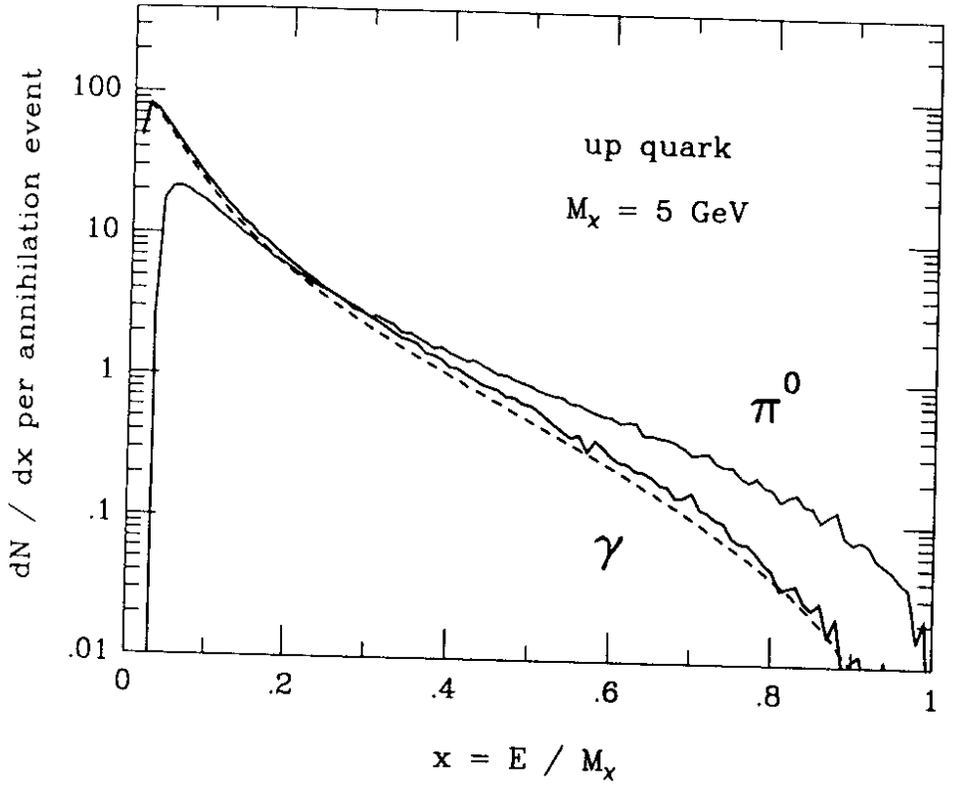

Figure 3a

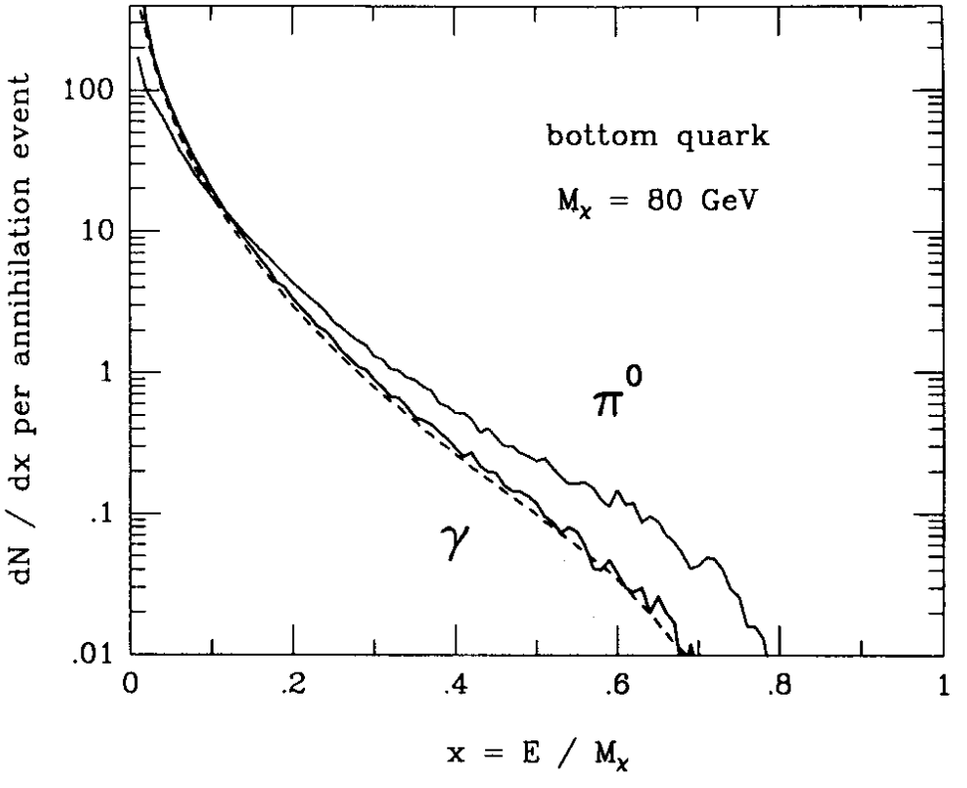

Figure 3b

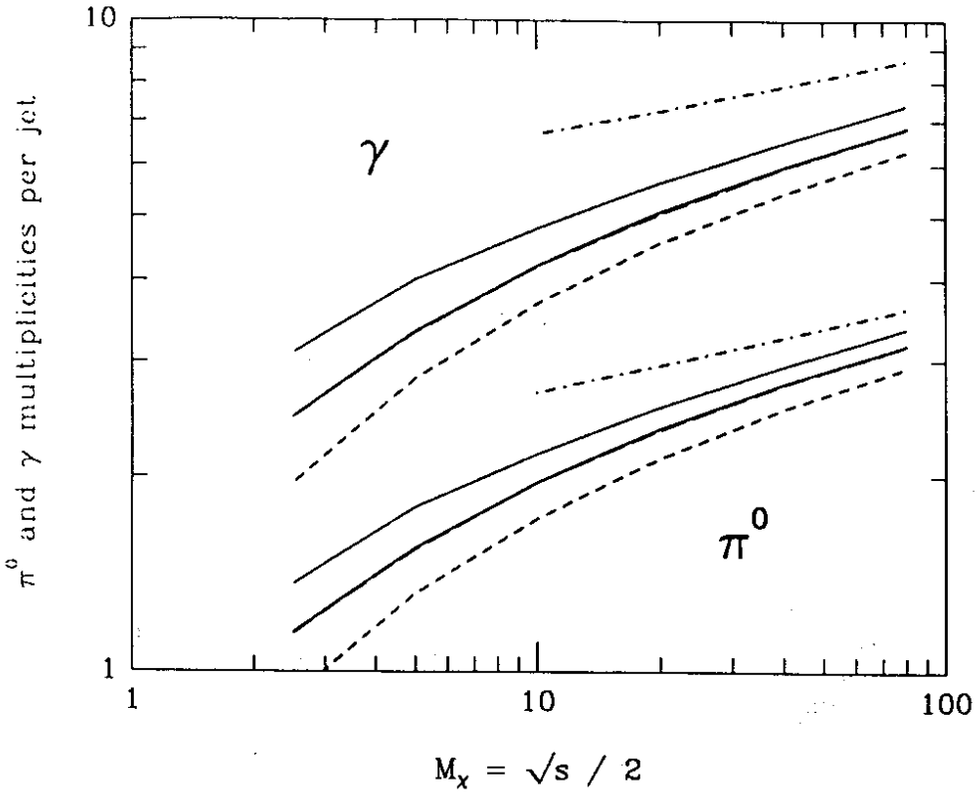

Figure 4a

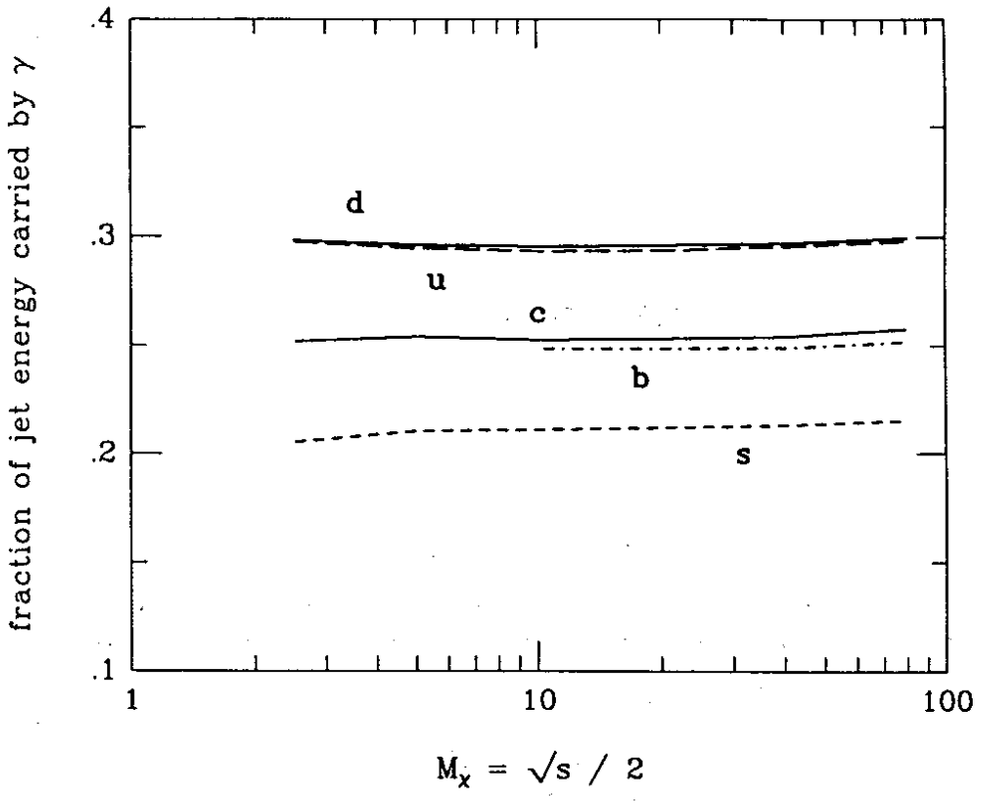

Figure 4b

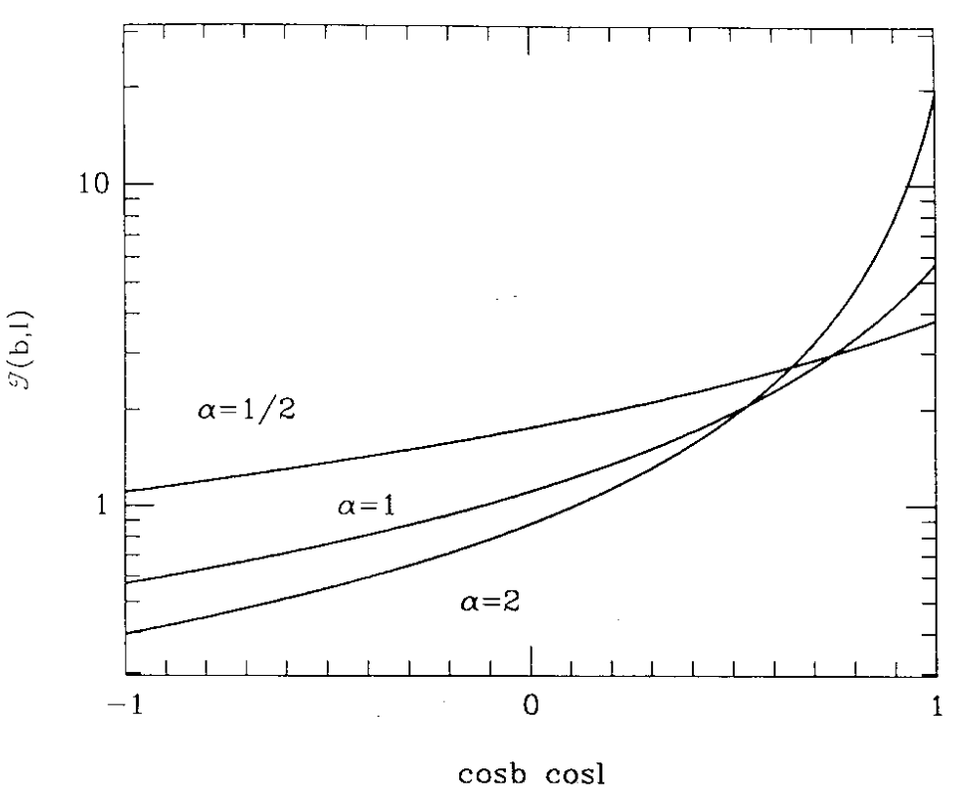

Figure 5

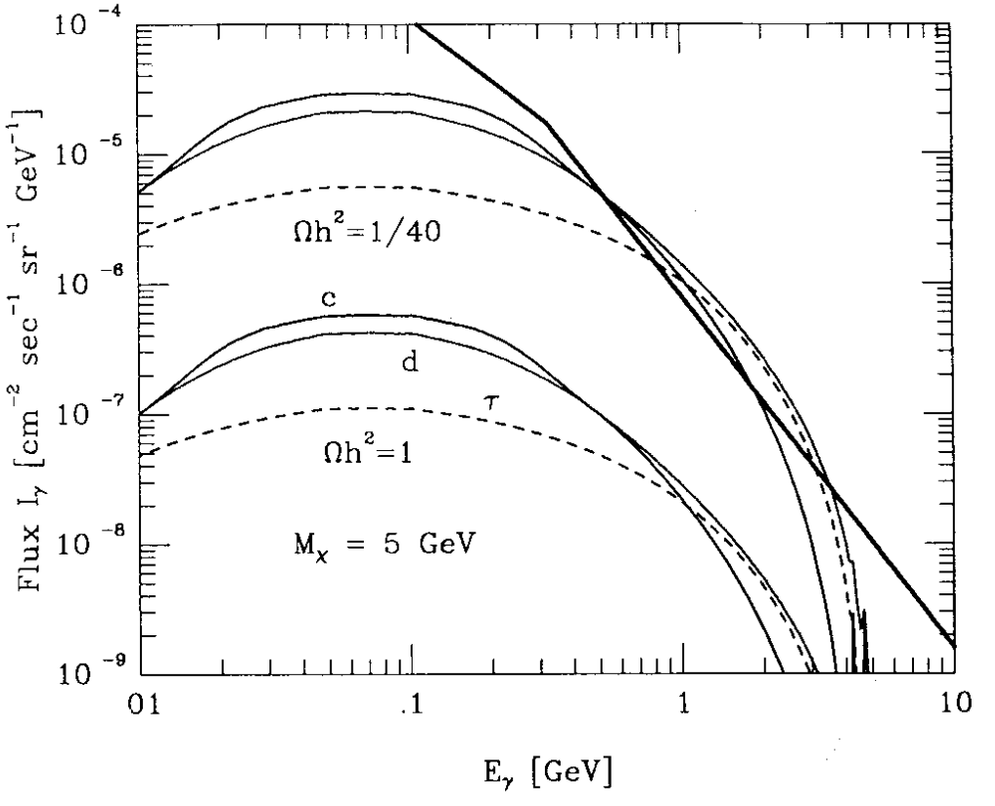

Figure 6a

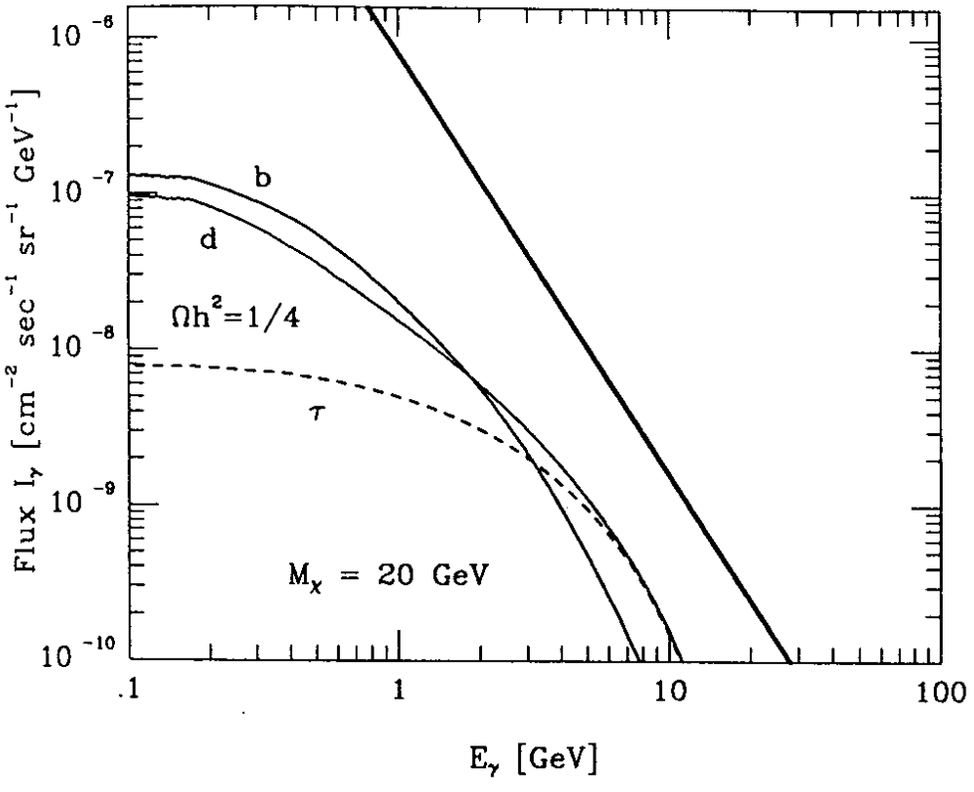

Figure 6b

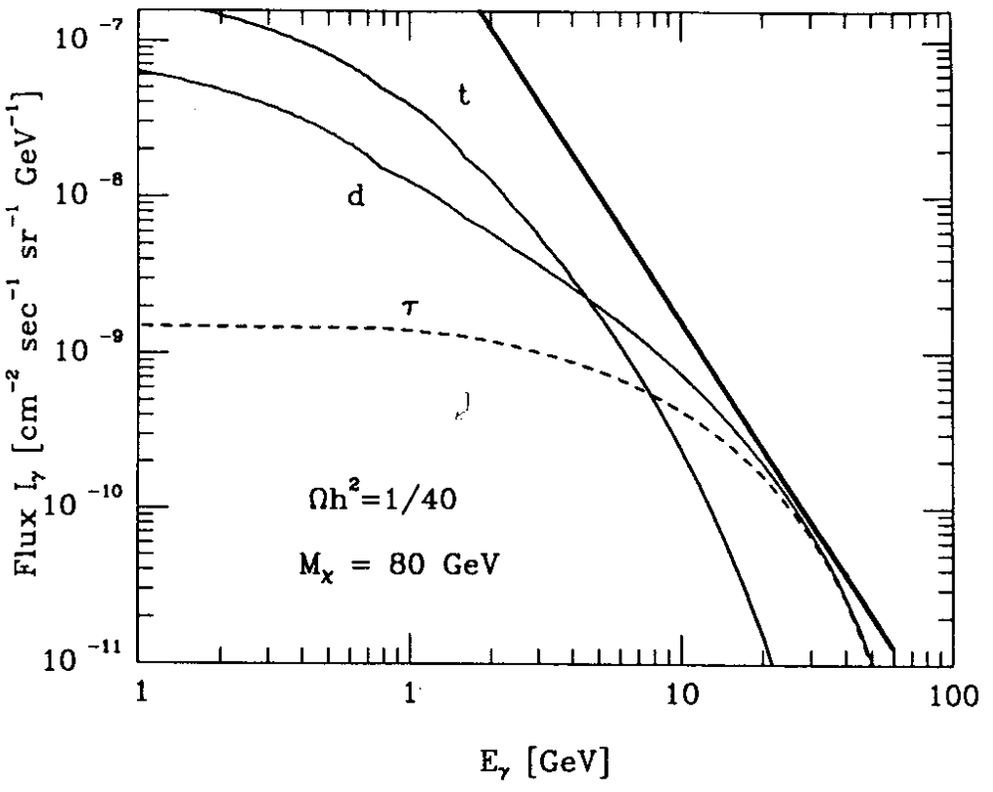

Figure 6c

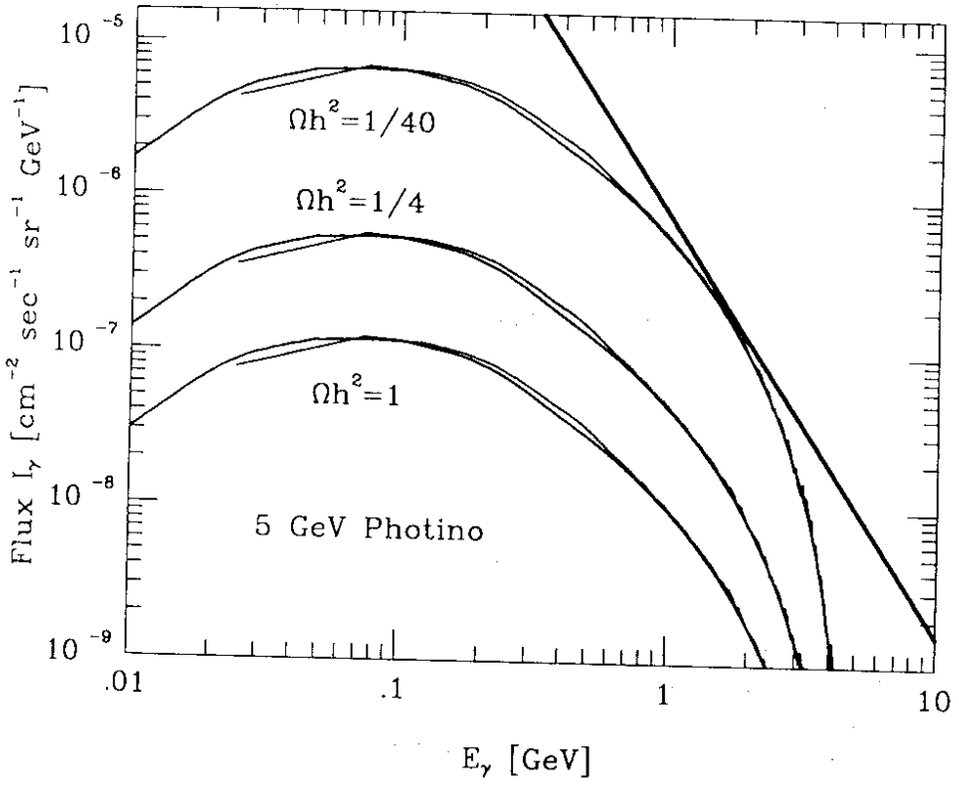

Figure 7a

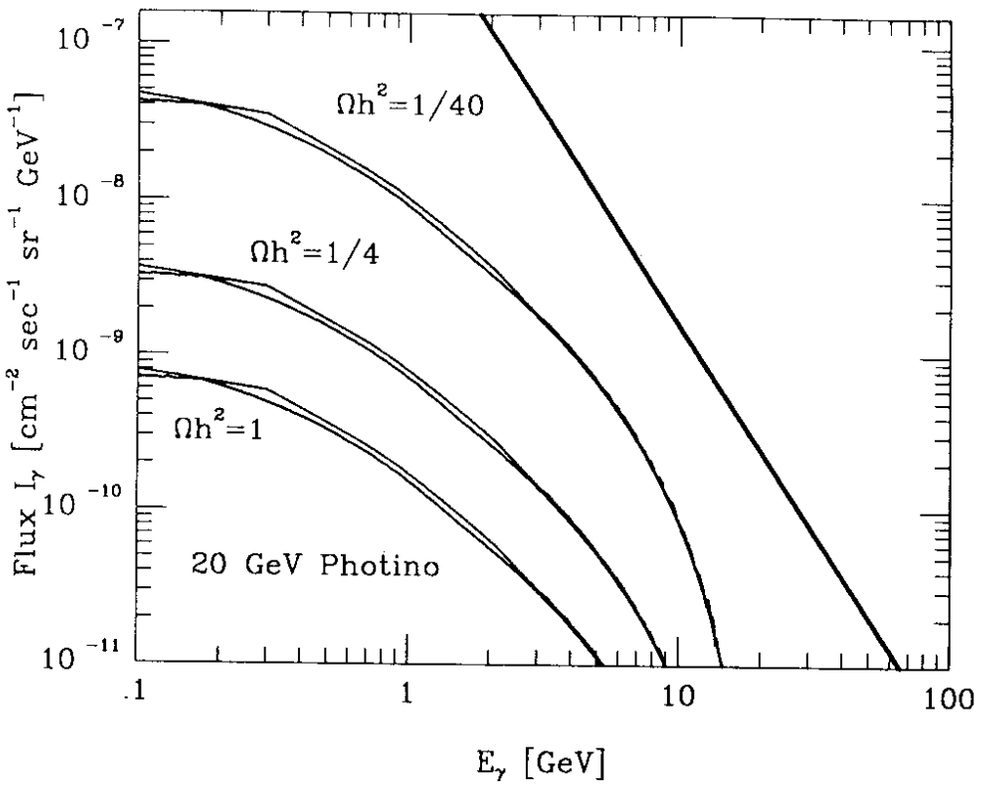

Figure 7b

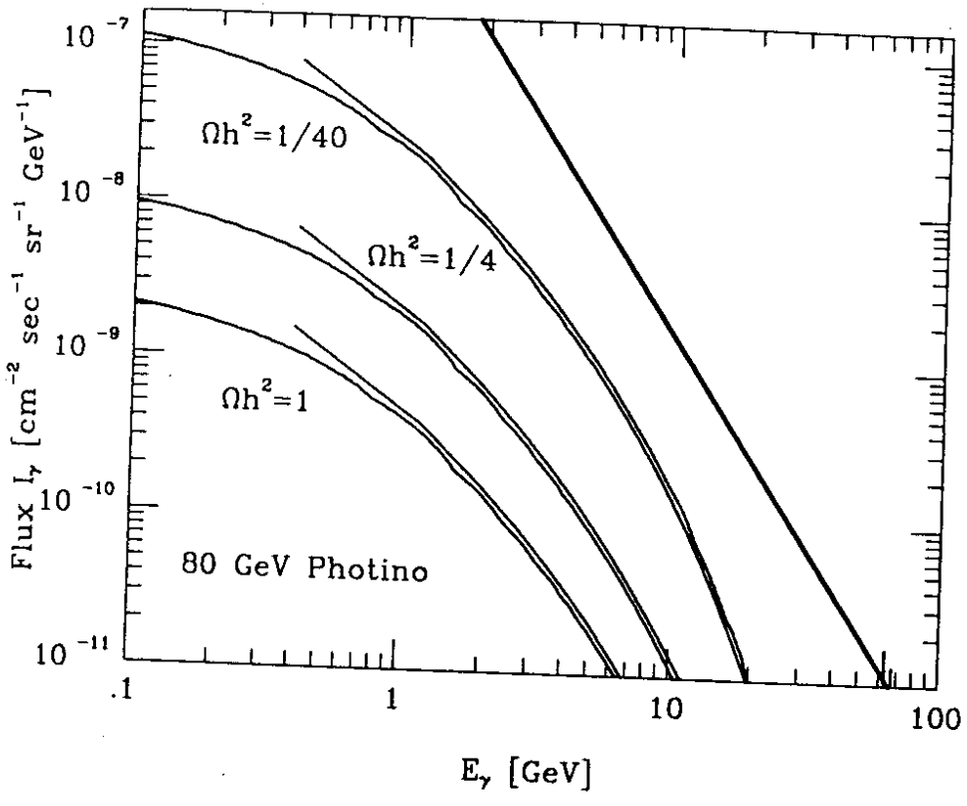
10^{-7}
10^{-8}
10^{-9}
10^{-10}
10^{-11}
$\Omega h^2=1/40$
$\Omega h^2=1/4$
$\Omega h^2=1$
80 GeV Photino
Flux I_γ [cm^{-2} sec^{-1} sr^{-1} GeV^{-1}]
.1
1
10
100
E_γ [GeV]

Figure 7c